

On the esterification reaction of phenacyl bromide with benzoic acids: microwave and ultrasound versus conventional heating

T. Erdogan*

Kocaeli University, Department of Chemistry and Chemical Processing Technologies, Kocaeli Vocational School, Kocaeli, Turkey

Submitted January 21, 2018; Revised February 1, 2019

In this study it was aimed to develop new experimental methods for the esterification reaction of phenacyl bromide with benzoic acids. For this purpose; ultrasound and microwave energy were used and the results showed that both sonication and microwave irradiation increase the effectiveness of the investigated esterification reaction. In the second part of the study, some DFT calculations with B3LYP method were performed and computational results were compared with the experimentally obtained data. All DFT calculations were performed at DFT B3LYP level of theory using 6-31G(d), 6-31G(d,p), 6-311G(d,p) and 6-311+G(2d,p) basis sets. NMR calculations were carried out using both CSGT and GIAO methods. MEP maps, FMOs, and Mulliken atomic charges were computationally determined with the same basis sets.

Keywords: Esterification, phenacyl benzoates, microwave chemistry, sonochemistry, computational chemistry

INTRODUCTION

Esterification reaction is one of the most fundamental reactions in organic chemistry and widely used in various areas such as pharmacology, polymer technology, flavor and fragrance industry etc. [1]. The literature contains various well-known esterification methods for the synthesis of various esters including phenacyl benzoates. Phenacyl benzoates can be synthesized via the reaction of phenacyl bromides and benzoic acids. Although, literature contains various methods for the reaction of phenacyl bromide with benzoic acid or terephthalaldehydic acid, these methods generally requires heating and/or long reaction times, so, it needs to be developed more effective and rapid methods. The extant literature contains several reports for the reaction of phenacyl bromide with benzoic acid [1-14] and for the reaction of phenacyl bromide with terephthalaldehydic acid [15] but none of these methods includes ultrasound or microwave energy. On the other hand, literature contains several reports on the microwave-assisted reaction of phenacyl bromide or substituted phenacyl bromides with substituted benzoic acids [16-19], however there is not an ultrasound-assisted method for these reactions, too.

In this study, it was postulated that the reaction between phenacyl bromide and benzoic acids could be accomplished in an efficient way by using ultrasound or microwave irradiation. In the present study, experimental studies have been focused on two different methods; one of them is ultrasound, and the other one is microwave-assisted method. To

the best of our knowledge, for the reactions of phenacyl bromide with benzoic acid and terephthalaldehydic acid, there is no study in the literature in which ultrasound and/or microwave energy were used. In these methods; phenacyl bromide (**2**) was reacted with benzoic acid (**3a**) and terephthalaldehydic acid (**3b**) under sonication or under microwave irradiation in the presence of sodium carbonate. The results show that both methods allow the investigated esterification reaction in good yields. Yields for the reactions are approximately 90% for benzoic acid and 80% for terephthalaldehydic acid. The reaction pathway is given in Fig. 1.

In the microwave-assisted method, 175 W of microwave energy was applied. It was observed that increasing microwave energy increases the reaction yield but 175 W is the maximum applicable microwave energy due to a sudden increase in boiling rate of the solvent system. On the other hand, the optimum reaction time was found to be 15 minutes. The reaction yield increases by increasing reaction time gradually but over 15 minutes there is not a considerable increase in the reaction yield. In the ultrasound-assisted method, it takes 30 minutes to consume all the reactants at 70°C. In these reaction conditions, the reaction yields of both methods are identical but the microwave-assisted method is faster than the ultrasound-assisted method. The results show that both of these methods are good alternatives to conventional heating because of the dramatically decreased reaction times. The methods in which conventional heating is used, it takes minimum 2 hours of refluxing to complete the

* To whom all correspondence should be sent

E-mail: taner.erdogan@kocaeli.edu.tr:

reaction. In the synthesis of phenacyl bromide (**2**) from acetophenone (**1**), a modified form of a literature procedure [20] was used.

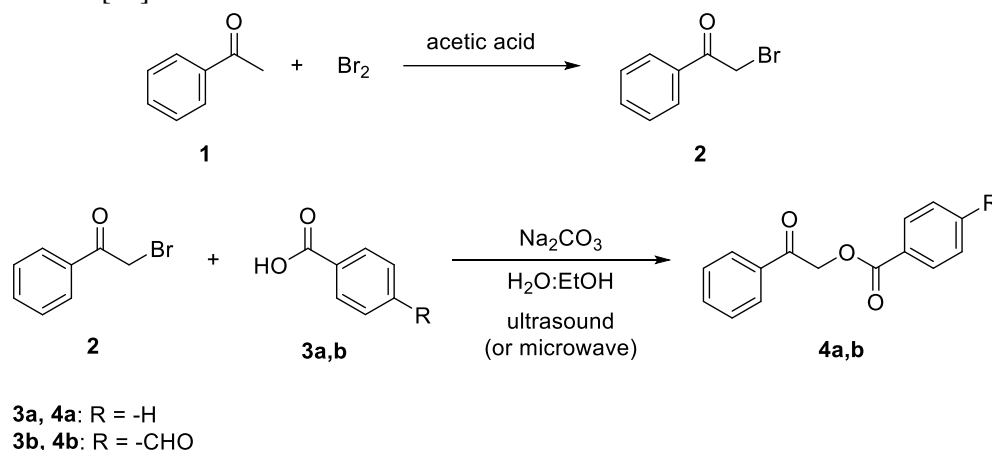


Fig. 1. Reaction pathway.

In the second part of the study, some DFT (Density Functional Theory) calculations have been performed on the investigated compounds and a comparison between experimental and computationally obtained data have been made. Geometry optimizations, frequency analysis and NMR calculations were carried out at B3LYP (Becke three-parameter hybrid functional combined with Lee-Yang-Parr correlation functional) level of theory using 6-31G(d), 6-31G(d,p), 6-311G(d,p), 6-311+G(2d,p) basis sets. In NMR calculations both GIAO (Gauge-Independent Atomic Orbital) and CSGT (Continuous Set of Gauge Transformations) methods were used. All computations have been performed using Gaussian 09. Revision D.01 [21] and Avogadro 1.1.1 [22] Program Packages, and GaussView5 [23] was used for the visualization of the computational results.

EXPERIMENTAL

Ultrasound-assisted reactions were carried out using Bandelin Sonorex ultrasonic bath. Microwave synthesis were carried out on CEM Discover SP Microwave System. NMR spectra were taken on Agilent Mercury 400. Melting points were determined using Barnstead Electrothermal 9100 melting point apparatus.

Synthesis of phenacyl bromide (**2**)

In the synthesis of phenacyl bromide; to an ice-cold solution of acetophenone (0.20 mol, 24 g) in acetic acid (100 mL), bromine (0.22 mol, 11.3 mL) was added dropwise in 30 minutes. The reaction mixture was stirred for additional 3 hours at room temperature then poured into crushed ice-water and formed solids were collected by filtration and recrystallized from ethanol.

Esterification reaction

Method A. Benzoic acid/terephthalaldehydic acid (5 mmol) and Na_2CO_3 (2.5 mmol, 0.265 g) were dissolved in water (5 mL), then phenacyl bromide (5 mmol, 1 g) and ethanol (10 mL) were added and the reaction mixture was placed in the ultrasonic bath and sonicated for 30 minutes at 70°C . After 30 minutes of sonication, reaction mixture was allowed to cool and formed solids were collected by filtration and recrystallized from ethanol.

Method B. Benzoic acid/terephthalaldehydic acid (5 mmol) and Na_2CO_3 (2.5 mmol, 0.265 g) were dissolved in water (5 mL), then phenacyl bromide (5 mmol, 1 g) and ethanol (10 mL) were added and the reaction mixture was placed in the microwave system and irradiated with 175 W of MW energy for 15 minutes. After 15 minutes of irradiation, reaction mixture was allowed to cool and formed solids were collected by filtration and recrystallized from ethanol.

2-oxo-2-phenylethyl benzoate (**4a**)

White solid, T_{mp} $113\text{-}115^\circ\text{C}$; ^1H NMR, δ , ppm: 5.58 s (2H, OCH_2CO), 7.54-7.44 m (4H, ArH), 7.65-7.57 m (2H, ArH), 7.97 d (2H, ArH, J 7.6 Hz), 8.15 d (2H, ArH, J 7.6 Hz); [Lit. [2], ^1H NMR, δ , ppm: 5.61 s (2H, OCH_2CO), 7.48-7.56 m (4H, ArH), 7.60-7.67 m (2H, ArH), 7.99-8.01 m (2H, ArH), 8.16-8.19 m (2H, ArH).

2-oxo-2-phenylethyl 2-phenylacetate (**4b**)

Light yellow solid, T_{mp} $108\text{-}110^\circ\text{C}$; ^1H NMR, δ , ppm: 5.62 s (2H, OCH_2CO), 7.48-7.54 m (2H, ArH), 7.60-7.64 m (1H, ArH), 7.94-8.00 m (4H, ArH), 8.30 d (2H, ArH, J 8.4 Hz), 10.12 s (1H, CHO); [Lit. [15], T_{mp} $106\text{-}109^\circ\text{C}$] ^1H NMR δ , ppm: 5.6 s (2H, OCH_2CO), 8.05 m (9H, ArH), 10.08 s (1H, CHO).

THEORETICAL CALCULATIONS

Single point energies for optimized structures

Single Point Energy (SPE) is the sum of nuclear repulsion energy and the electronic energy of the molecule at the specified nuclear configuration. A single point energy calculation is a prediction of the

energy and related properties for a molecule with a specified geometric structure. [25] SPEs were determined for the optimized structures at DFT B3LYP level of theory using 6-31G(d), 6-31G(d,p), 6-311G(d,p) and 6-311+G(2d,p) basis sets. Energies for **1**, **2**, **3a**, **3b**, **4a** and **4b** are given in Table 1.

Table 1. Calculated single point energies of the compounds.

Compound	opt1 ^a (eV)	opt2 ^b (eV)	opt3 ^c (eV)	opt4 ^d (eV)
1	-10473.56	-10473.89	-10476.27	-10476.71
2	-80436.76	-80437.06	-80505.83	-80506.15
3a	-11451.16	-11451.52	-11454.35	-11454.88
3b	-14534.82	-14535.18	-14538.83	-14539.52
4a	-21891.77	-21892.28	-21897.36	-21898.28
4b	-24975.45	-24975.95	-24981.85	-24982.94

^a B3LYP/6-31G(d) ^b B3LYP/6-31G(d,p) ^c B3LYP/6-311G(d,p) ^d B3LYP/6-311+G(2d,p)

Optimized structure analysis

Optimized structures and geometric parameters were determined computationally at DFT B3LYP level of theory using 6-31G(d), 6-31G(d,p), 6-311G(d,p) and 6-311+G(2d,p) basis sets. Optimized structures of **4a** and **4b**, calculated with 6-311+G(2d,p) basis set, are given in Fig. 2 and Fig. 3, respectively. Tables 2, 3 and 4 represent selected

bond lengths and bond angles of **4a** and **4b** calculated at B3LYP/6-311+G(2d,p) level of theory and the experimental values. The experimental values have been obtained from the literature. [26] Except for some certain bonds and bond angles, it can be seen that the errors are less than 1% for bond lengths and less than 5% for bond angles. It was also observed that larger basis sets estimate the bond lengths and bond angles more accurately.

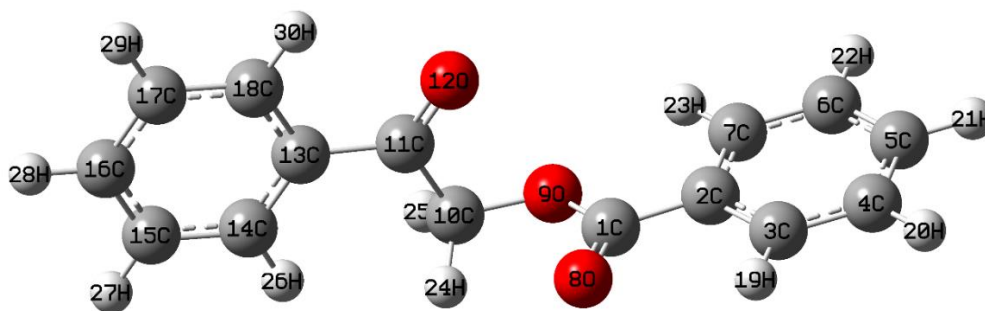


Fig. 2. Optimized structure of **4a**

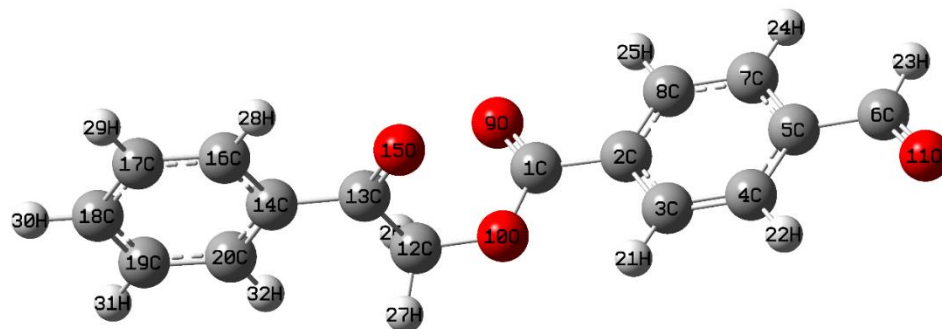
Table 2. Selected experimental and calculated bond lengths for **4a**.

Atoms	Bond Length (Exp. ^a) [Å]	Bond Length (Calc. ^b) [Å]
13C-11C	1.481	1.495
11C-12O	1.205	1.210
11C-10O	1.481	1.532
10C-9O	1.441	1.420
9O-1C	1.357	1.358
1C-8O	1.197	1.207
1C-2C	1.482	1.487

^a Lit. [26]
^b B3LYP/6-311+G(2d,p)

Table 3. Selected experimental and calculated bond angles for **4a**.

Atoms	Bond Angle (Exp. ^a) [°]	Bond Angle (Calc. ^b) [°]
13C-11C-12O	122.2	122.0
13C-11C-10C	118.0	117.7
12O-11C-10C	119.7	120.3
11C-10C-9O	112.4	111.4
10C-9O-1C	114.6	116.0
9O-1C-8O	122.5	122.9
8O-1C-2C	124.3	124.7

^a Lit. [26]^b B3LYP/6-311+G(2d,p)**Fig. 3.** Optimized structure of **4b**.**Table 4.** Selected geometric parameters for **4b**.

Atoms	Bond Length [Å] ^a	Atoms	Bond Angle [Å] ^a
13C-15O	1.210	2C-1C-9O	124.3
13C-14C	1.493	2C-1C-10O	112.3
12C-13C	1.533	9O-1C-10O	123.3
10O-12C	1.422	1C-10O-12C	116.0
10O-1C	1.354	10O-12C-13C	111.3
1C-9O	1.207	12C-13C-15O	120.2
1C-2C	1.491	12C-13C-14C	117.7
		15O-13C-14C	122.1

^a B3LYP/6-311+G(2d,p)

Frequency analysis

Frequency analysis were also carried out at DFT B3LYP level of theory using 6-31G(d), 6-31G(d,p), 6-311G(d,p) and 6-311+G(2d,p) basis sets. Experimental and calculated infrared spectra of **4a** and **4b** are given in Figs. 4 and 5, respectively. For the calculated infrared spectra a scale factor (0.9680) was applied. It was also observed that larger basis sets estimate IR spectra of the investigated molecules more accurately.

NMR spectral analysis

Nuclear magnetic shield tensors were computationally determined at DFT B3LYP level of theory using 6-31G(d), 6-31G(d,p), 6-311G(d,p) and 6-311+G(2d,p) basis sets with GIAO (Gauge-Independent Atomic Orbital) and CSGT (Continuous Set of Gauge Transformations) methods. Calculated and experimental ¹H NMR data of **4a** and **4b** are given in Tables 5, 6, 7 and 8. It can be seen that the best results were obtained at GIAO 6-31G(d,p) and CSGT 6-311+G(2d,p) levels. It was also observed that in the CSGT type NMR calculations, larger basis sets estimate the chemical

shifts more accurately, on the other hand in the GIAO type NMR calculations, larger basis sets overestimate the chemical shifts.

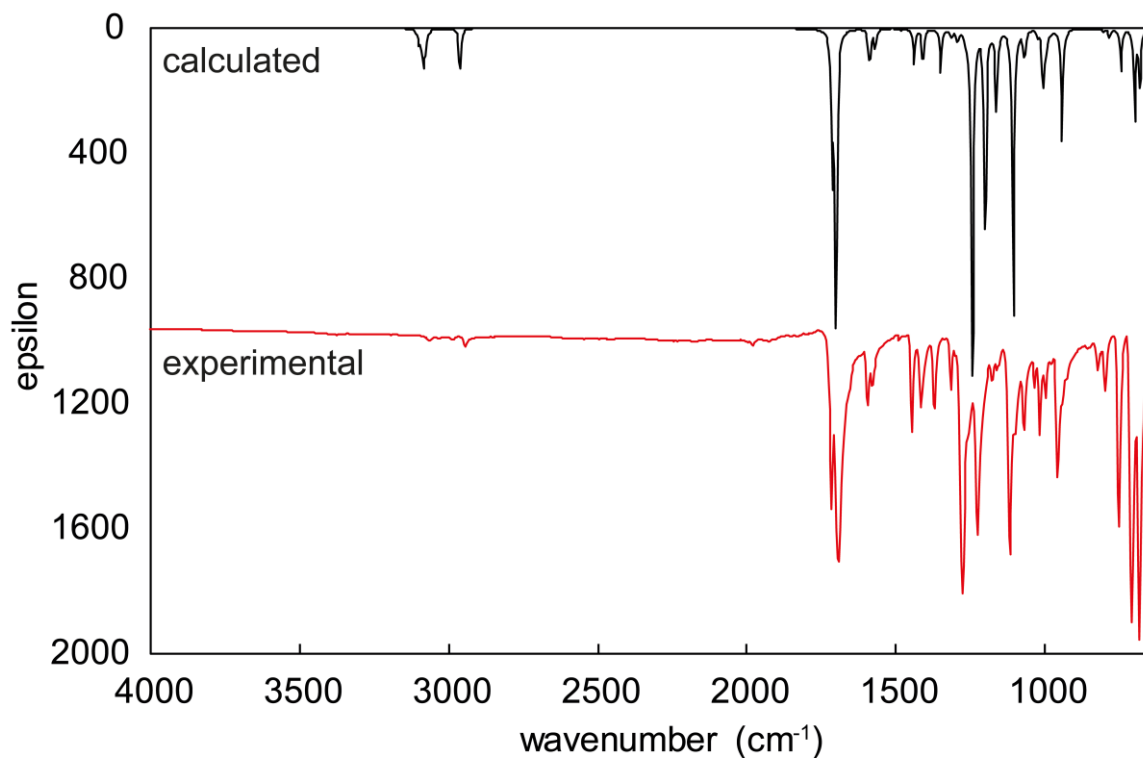


Fig. 4. Experimental and calculated infrared spectra of 4a

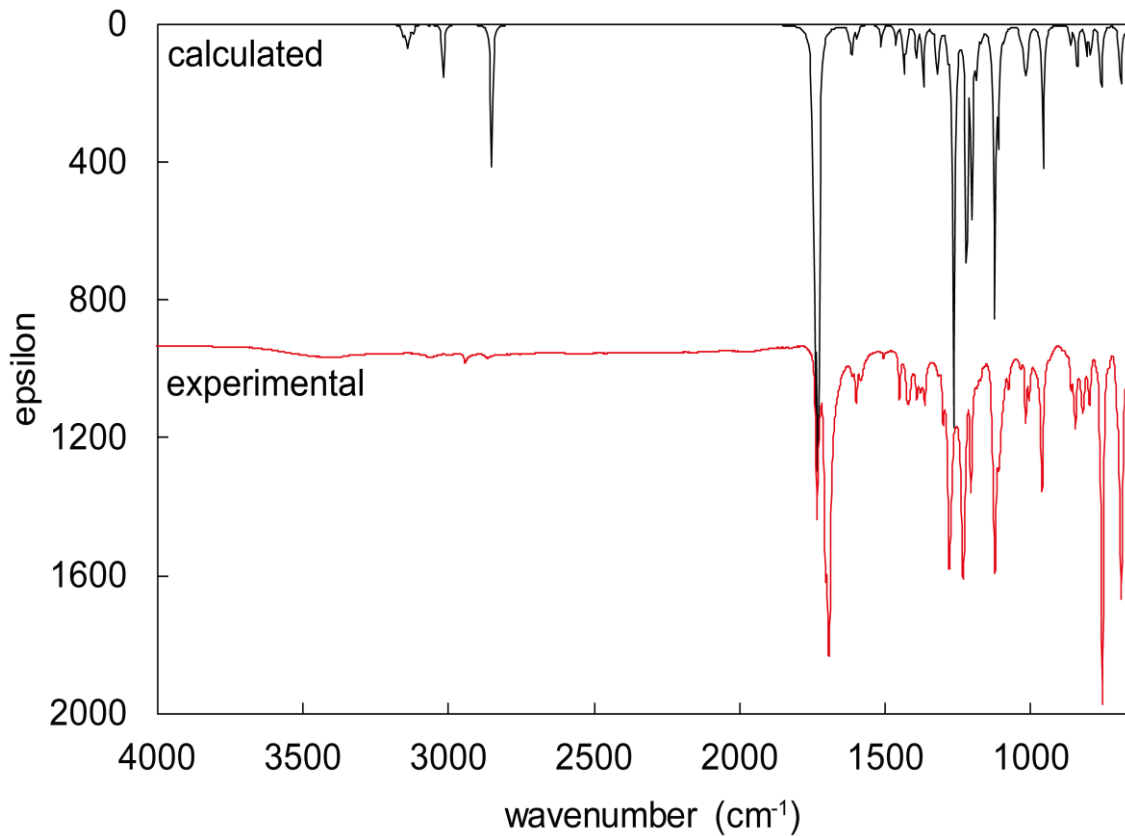


Fig. 5. Experimental and calculated infrared spectra of 4b.

Table 5. Experimental and calculated ^1H NMR chemical shifts for **4a** (CSGT).

Comp.	Exp.	csgt1 ^a	csgt2 ^b	csgt3 ^c	csgt4 ^d
19H	8.15	5.22	5.80	6.98	8.23
23H	8.15	5.22	5.80	6.98	8.23
26H	7.97	4.93	5.52	6.73	8.02
30H	7.97	4.93	5.52	6.73	8.02
28H	7.65-7.57	4.82	5.38	6.51	7.50
21H	7.65-7.57	4.85	5.39	6.52	7.52
27H	7.54-7.44	4.75	5.31	6.45	7.38
29H	7.54-7.44	4.75	5.31	6.45	7.38
20H	7.54-7.44	4.77	5.32	6.47	7.42
22H	7.54-7.44	4.77	5.32	6.47	7.42
24H	5.58	2.90	3.43	4.26	5.49
25H	5.58	2.90	3.43	4.26	5.49

^a B3LYP/6-31G(d) ^b B3LYP/6-31G(d,p) ^c B3LYP/6-311G(d,p) ^d B3LYP/6-311+G(2d,p)

Table 6. Experimental and calculated ^1H NMR chemical shifts for **4a** (GIAO).

Comp.	Exp.	giao1 ^a	giao2 ^b	giao3 ^c	giao4 ^d
19H	8.15	8.13	8.38	8.48	8.62
23H	8.15	8.13	8.38	8.48	8.62
26H	7.97	7.87	8.12	8.22	8.40
30H	7.97	7.87	8.12	8.22	8.40
28H	7.65-7.57	7.40	7.59	7.71	7.85
21H	7.65-7.57	7.38	7.56	7.67	7.77
27H	7.54-7.44	7.32	7.52	7.64	7.69
29H	7.54-7.44	7.32	7.52	7.64	7.69
20H	7.54-7.44	7.29	7.48	7.59	7.68
22H	7.54-7.44	7.29	7.48	7.59	7.68
24H	5.58	5.26	5.44	5.58	5.76
25H	5.58	5.26	5.44	5.58	5.76

^a B3LYP/6-31G(d) ^b B3LYP/6-31G(d,p) ^c B3LYP/6-311G(d,p) ^d B3LYP/6-311+G(2d,p)

Table 7. Experimental and calculated ^1H NMR chemical shifts for **4b** (CSGT).

Comp.	Exp.	csgt1 ^a	csgt2 ^b	csgt3 ^c	csgt4 ^d
23-H	10.12	6.60	7.38	8.82	10.26
21-H	8.30	5.32	5.94	7.12	8.32
25-H	8.30	5.32	5.94	7.12	8.32
28-H	8.00-7.94	4.92	5.51	6.71	7.85
32-H	8.00-7.94	4.92	5.51	6.71	7.85
22-H	8.00-7.94	4.96	5.54	6.73	8.01
24-H	8.00-7.94	4.96	5.54	6.73	8.01
30-H	7.66-7.60	4.85	5.40	6.54	7.55
29-H	7.54-7.48	4.76	5.33	6.49	7.43
31-H	7.54-7.48	4.76	5.33	6.49	7.43
26-H	5.62	2.92	3.46	4.28	5.51
27-H	5.62	2.92	3.46	4.28	5.51

^a B3LYP/6-31G(d) ^b B3LYP/6-31G(d,p) ^c B3LYP/6-311G(d,p) ^d B3LYP/6-311+G(2d,p)

Table 8. Experimental and calculated ^1H NMR chemical shifts for **4b** (GIAO).

Comp.	Exp.	giao1 ^a	giao2 ^b	giao3 ^c	giao4 ^d
23-H	10.12	9.99	10.15	10.34	10.65
21-H	8.30	8.25	8.50	8.59	8.73
25-H	8.30	8.25	8.50	8.59	8.73
28-H	8.00-7.94	7.88	8.13	8.22	8.38
32-H	8.00-7.94	7.88	8.13	8.22	8.38
22-H	8.00-7.94	7.80	8.02	8.11	8.22
24-H	8.00-7.94	7.80	8.02	8.11	8.22
30-H	7.66-7.60	7.40	7.60	7.71	7.78
29-H	7.54-7.48	7.34	7.53	7.64	7.74
31-H	7.54-7.48	7.34	7.53	7.64	7.74
26-H	5.62	5.31	5.48	5.61	5.81
27-H	5.62	5.31	5.48	5.61	5.81

^a B3LYP/6-31G(d) ^b B3LYP/6-31G(d,p) ^c B3LYP/6-311G(d,p) ^d B3LYP/6-311+G(2d,p)

Molecular electrostatic potential maps

Molecular electrostatic potential (MEP) map gives information about the electron rich and electron deficient parts of the investigated molecule. MEP maps were calculated at DFT B3LYP/6-31G(d), B3LYP/6-311G(d,p) and B3LYP/6-

311+G(2d,p) levels of theory. Calculated MEP diagrams of **3a**, **3b**, **4a** and **4b** are given in Fig. 6. For **3a** and **3b**, it can be seen that negative charge was dominantly located on the carbonyl group and partially on the hydroxyl group of carboxylic acid. For **4a** and **4b**, negative charge was located on the carbonyl and ester functional groups.

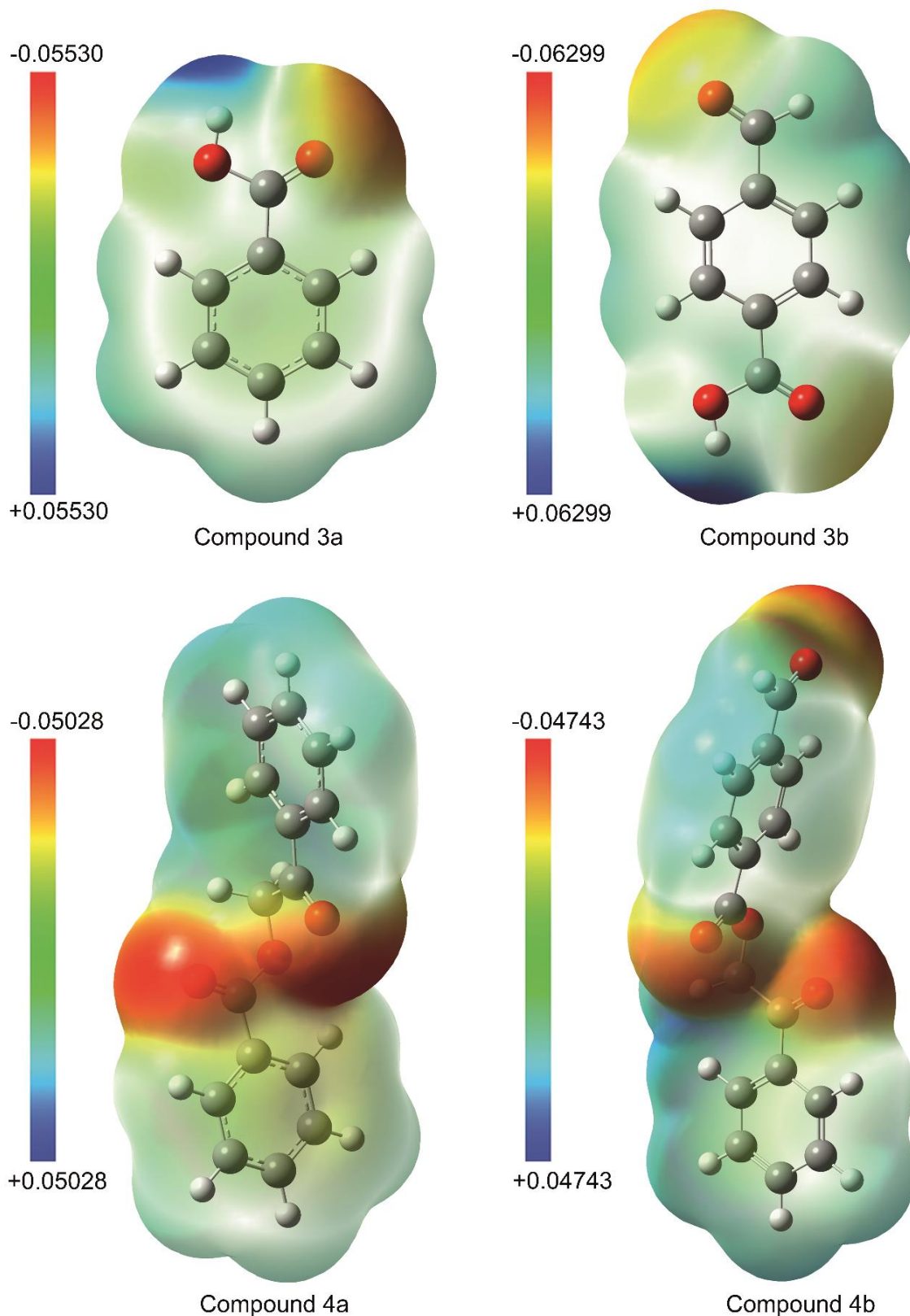


Fig. 6. MEP map diagrams of 3a, 3b, 4a and 4b.

Frontier molecular orbitals and global reactivity descriptors

Lowest unoccupied molecular orbital (LUMO) and the highest occupied molecular orbital (HOMO)

energy calculations were carried out at DFT B3LYP level of theory using 6-31G(d), 6-31G(d,p), 6-311G(d,p) and 6-311+G(2d,p) basis sets.. Ionization potential (I), electron affinity (A), electronegativity (χ), chemical hardness (η), chemical softness (S),

electronic chemical potential (μ) and electrophilicity index (ω) values were determined and are given in Tables 9, 10, 11 and 12. Ionization potential can be calculated using Eqn. (1) and corresponds to a minimum energy required to remove an electron from an atom or molecule and electron affinity can be calculated using Eqn. (2). [27] and corresponds to the energy released when an electron is added to a neutral atom or molecule in the gaseous state. On the other hand, electronegativity, chemical hardness, chemical softness, electronic chemical potential and electrophilic index can be calculated using Eqns. (3-7). [28-34].

$$I = -E_{HOMO} \quad (1)$$

$$A = -E_{LUMO} \quad (2)$$

$$\chi = (I + A)/2 \quad (3)$$

$$\eta = (I - A)/2 \quad (4)$$

$$S = 1/\eta \quad (5)$$

$$\mu = -(I + A)/2 \quad (6)$$

$$\omega = \mu^2/2\eta \quad (7)$$

Table 9. Global reactivity descriptors for **3a**.

Entry	opt1 ^a	opt2 ^b	opt3 ^c	opt4 ^d
LUMO	-1.309	-1.314	-1.568	-1.783
HOMO	-7.087	-7.094	-7.336	-7.453
Gap	5.778	5.780	5.769	5.670
<i>I</i>	7.087	7.094	7.336	7.453
<i>A</i>	1.309	1.314	1.568	1.783
χ	4.198	4.204	4.452	4.618
η	2.889	2.890	2.884	2.835
<i>S</i>	0.346	0.346	0.347	0.353
μ	-4.198	-4.204	-4.452	-4.618
ω	3.051	3.058	3.436	3.761

^a B3LYP/6-31G(d) ^b B3LYP/6-31G(d,p) ^c B3LYP/6-311G(d,p) ^d B3LYP/6-311+G(2d,p)

Table 10. Global reactivity descriptors for **3b**.

Entry	opt1 ^a	opt2 ^b	opt3 ^c	opt4 ^d
LUMO	-2.414	-2.417	-2.637	-2.848
HOMO	-7.230	-7.225	-7.444	-7.609
Gap	4.816	4.809	4.808	4.760
<i>I</i>	7.230	7.225	7.444	7.609
<i>A</i>	2.414	2.417	2.637	2.848
χ	4.822	4.821	5.041	5.228
η	2.408	2.404	2.404	2.380
<i>S</i>	0.415	0.416	0.416	0.420
μ	-4.822	-4.821	-5.041	-5.228
ω	4.828	4.833	5.284	5.742

^a B3LYP/6-31G(d) ^b B3LYP/6-31G(d,p) ^c B3LYP/6-311G(d,p) ^d B3LYP/6-311+G(2d,p)

Chemical hardness is a measure of the resistance of a compound to change in its electronic configuration. [35] Chemical hardness values of compounds showed similar trend to the HOMO-LUMO gap values. It can be seen that chemical

hardness of **3a** is bigger than **3b** and **4a** is bigger than **4b**. Electrophilicity index is considered to be a measure of electrophilic power. [27] A good electrophile is characterized by a high value of electrophilicity index, in opposite, lower values

correspond to good nucleophiles. It was found that the electrophilicity index of **3a** is lower than the electrophilicity index of **3b** and the electrophilicity

index of **4a** is lower than the electrophilicity index of **4b**.

Table 11. Global reactivity descriptors for **4a**.

Entry	opt1 ^a	opt2 ^b	opt3 ^c	opt4 ^d
LUMO	-1.648	-1.657	-1.906	-2.056
HOMO	-6.880	-6.887	-7.125	-7.228
Gap	5.232	5.230	5.219	5.171
<i>I</i>	6.880	6.887	7.125	7.228
<i>A</i>	1.648	1.657	1.906	2.056
χ	4.264	4.272	4.516	4.642
η	2.616	2.615	2.609	2.586
<i>S</i>	0.382	0.382	0.383	0.387
μ	-4.264	-4.272	-4.516	-4.642
ω	3.476	3.489	3.908	4.167

^a B3LYP/6-31G(d) ^b B3LYP/6-31G(d,p) ^c B3LYP/6-311G(d,p) ^d B3LYP/6-311+G(2d,p)

Table 12. Global reactivity descriptors for **4b**.

Entry	opt1 ^a	opt2 ^b	opt3 ^c	opt4 ^d
LUMO	-2.245	-2.253	-2.468	-2.642
HOMO	-7.089	-7.088	-7.304	-7.447
Gap	4.844	4.835	4.836	4.804
<i>I</i>	7.089	7.088	7.304	7.447
<i>A</i>	2.245	2.253	2.468	2.642
χ	4.667	4.670	4.886	5.045
η	2.422	2.417	2.418	2.402
<i>S</i>	0.413	0.414	0.414	0.416
μ	-4.667	-4.670	-4.886	-5.045
ω	4.496	4.512	4.937	5.297

^a B3LYP/6-31G(d) ^b B3LYP/6-31G(d,p) ^c B3LYP/6-311G(d,p) ^d B3LYP/6-311+G(2d,p)

Mulliken atomic charges

The Mulliken charge distribution over the atoms affects the molecular polarizability, electronic structure, dipole moment etc. In the computational studies, the Mulliken charge distribution of the synthesized molecules were determined at DFT B3LYP/6-31G(d), B3LYP/6-31G(d,p), B3LYP/6-311G(d,p) and B3LYP/6-311+G(2d,p) levels of theory. The Mulliken atomic charges for **4a** and **4b** at B3LYP/6-311+G(2d,p) level of theory are given in Figs. 7 and 8, respectively. In **4a** and **4b**, all oxygen atoms possess negative Mulliken charges, but the charges of the carbonyl oxygens are more negative. In **4a**, all carbon atoms have negative charge except 2C, 11C, 13C and 18C. In **4b**, all

carbonyl carbons (6C, 1C, 13C), ring carbons adjacent to carbonyl carbons (5C, 2C, 14C) and 16C have positive Mulliken charges.

RESULTS AND DISCUSSION

In this work, two novel methods have been proposed for the esterification reaction of phenacyl bromide with benzoic acid/terephthalaldehydic acid. The proposed methods allow investigated esterification reaction in good yields. Yields for the reactions are approximately 90% for benzoic acid and 80% for terephthalaldehydic acid.

In the esterification reaction, it was found that the yield of the reaction of phenacyl bromide with benzoic acid is higher than the yield of the reaction

of phenacyl bromide with terephthalaldehydic acid. This can be explained by the higher nucleophilic character of benzoic acid than that of terephthalaldehydic acid. Computational results also

support this situation. It can be seen from Tables 9 and 10 that the electrophilicity index (ω) of the terephthalaldehydic acid is higher than that of the benzoic acid.

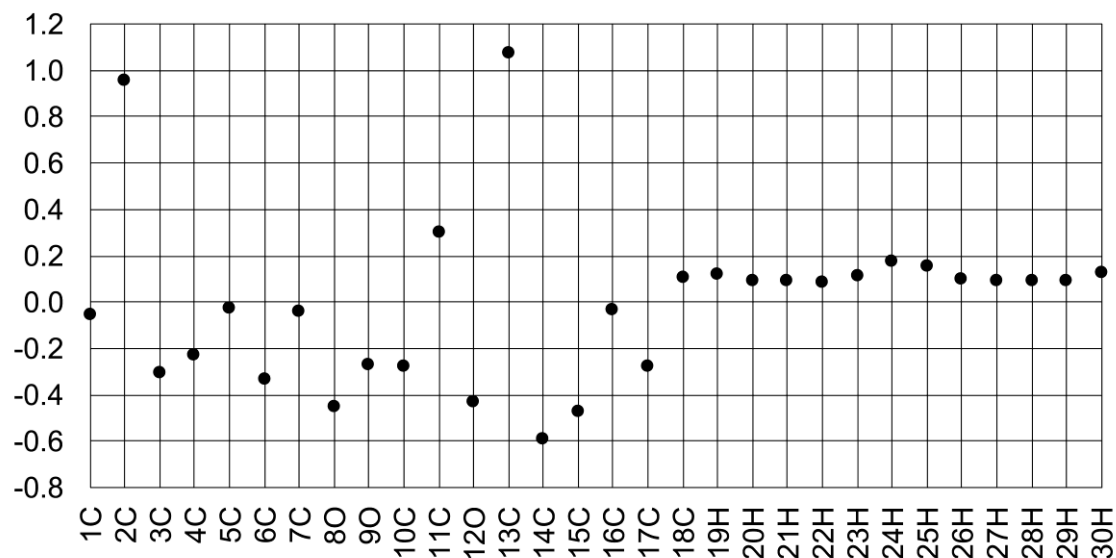


Fig. 7. Mulliken atomic charges of 4a.

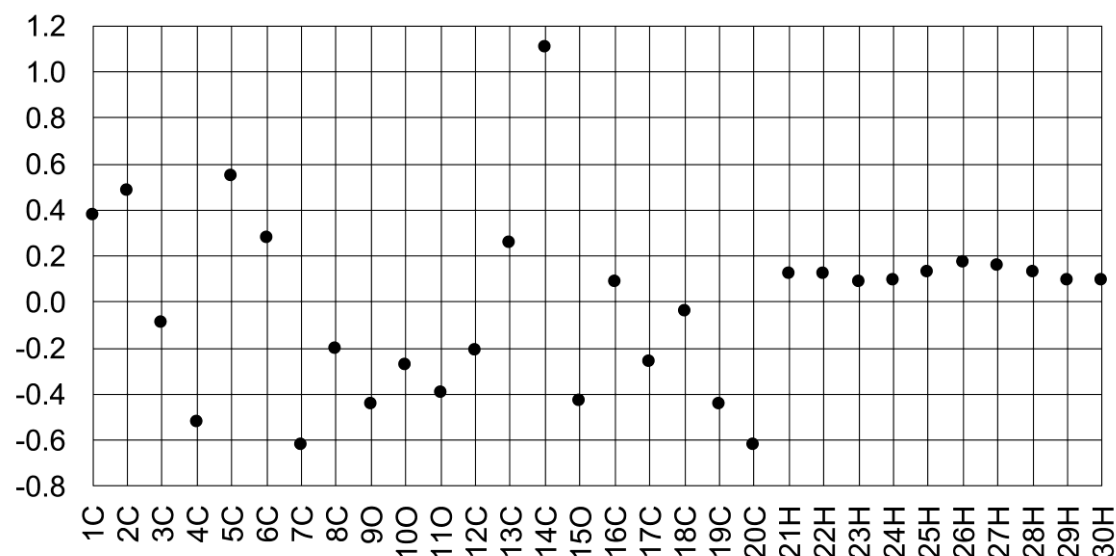


Fig. 8. Mulliken atomic charges of 4b.

In NMR calculations, it was found that the ^1H NMR chemical shifts obtained from calculations at DFT B3LYP/6-31G(d,p) GIAO and at DFT B3LYP/6-311+G(2d,p) CSGT levels of theory showed good agreement with the experimental results. Similar results have been obtained in a previous study [24]. It was also observed that in general, GIAO method is more successful than CSGT method and the accuracy of the CSGT method increases with the use of larger basis sets. In our study, successful results can only be obtained with 6-311+G(2d,p) basis set for CSGT method. On the other hand, GIAO method provide acceptable results with relatively small basis sets. Relatively

larger basis sets with GIAO method generally overestimates the ^1H NMR chemicals shifts.

In the microwave-assisted reactions, both pressure controlled closed system and atmospheric system were used. In the closed system, probably due to the increasing pressure inside the reactor, byproduct formation and as a result of this, decrease in the reaction yield was observed. It can be said that atmospheric focused microwave system is more suitable for the investigated reaction conditions.

Acknowledgements. This work was supported by Kocaeli University Scientific Research Projects Unit. Project Numbers: 2011/062; 2017/38 HD. The

author acknowledge Kocaeli University for the financial support.

REFERENCES

1. S.N. Dighe, R.V. Bhattad, R.R. Kulkarni, K.S. Jain, K.V. Srinivasan, *Synth. Commun.*, **40**, 3522 (2010).
2. Liu, S. Feng, C. Li, *ACS Sustainable Chem. Eng.*, **4**, 6754 (2016).
3. J. Chen, D. Liu, N. Butt, C. Li, D. Fan, Y. Liu, W. Zhang, *Angew. Chem., Int. Ed.*, **52**, 11632 (2013).
4. X. Zou, Y. Zhao, H. Cheng, Patent CN104803816A, 2015.
5. Y. Hu, J. Chen, Z.G. Le, Z.C. Chen and Q.G. Zheng, *Chin. Chem. Lett.*, **16**, 903 (2005).
6. Z. Huang, L. Xie and X. Huang, *Synth. Commun.*, **18**, 1167 (1988).
7. M. Inoue, M. Yamashita, Patent JP2008088128A, 2008.
8. M. Narender, M. Reddy, V. Kumar, K. Rao, *Synth. Commun.*, **35**, 1681 (2005).
9. J.H. Clark, J.M. Miller, *Tetrahedron Lett.*, 599 (1977).
10. R. Ruzicka, M. Zabadal, P. Klan, *Synth. Commun.*, **32**, 2581 (2002).
11. A.C. Giddens, Thesis, University of Auckland, 2008.
12. J. Chen, Z. Zhang, D. Liu and W. Zhang, *Angew. Chem., Int. Ed.*, **55**, 8444 (2016).
13. O. Noboru, Y. Takashi, S. Tadashi, T. Kazuhiko, K. Aritsune, *Bull. Chem. Soc. Japan*, **51**, 2404 (1978).
14. M. Thorat, R. Mane, M. Jagdale, M. Salunkhe, *Org. Prep. Proced. Int.*, **18**, 203 (1986).
15. J.S. Lindsey, I.C. Schreiman, H.C. Hsu, P.C. Kearney, A.M. Marguerettaz, *J. Org. Chem.*, **52**, 827 (1987).
16. Z. Li, Z.J. Quan, X.C. Wang, *Chem. Papers-Chemicke Zvesti*, **58**, 256 (2004).
17. M.M. Heravi, H.A. Oskooic, L. Bahrami, M. Ghassemzadeh, *Ind. J. Chem., Section B-Organic Chemistry Including Medicinal Chemistry*, **45**, 779 (2006).
18. S. Tasler, M. Kraus, S. Pegoraro, A. Aschenbrenner, E. Poggesi, R. Testa, G. Motta, A. Leonardi, *Bioorg. Med. Chem. Lett.*, **15**, 2876 (2005).
19. Y.H. Zhao, M.J. Luo, H.W. Liu, L.H. Wu, *Synth. Commun.*, **45**, 857 (2015).
20. L.P. Sidorova, T.A. Tseitler, V.V. Emel'yanov, E.A. Savateeva, N.E. Maksimova, N.N. Mochul'skaya, V.A. Chereshev, O.N. Chupakhin, *Pharm. Chem. J.*, **51**, 9 (2017).
21. M.J. Frisch, G.W. Trucks, H.B. Schlegel, G.E. Scuseria, M.A. Robb, J.R. Cheeseman, G. Scalmani, V. Barone, B. Mennucci, G.A. Petersson, H. Nakatsuji, M. Caricato, X. Li, H.P. Hratchian, A.F. Izmaylov, J. Bloino, G. Zheng, J.L. Sonnenberg, M. Hada, M. Ehara, K. Toyota, R. Fukuda, J. Hasegawa, M. Ishida, T. Nakajima, Y. Honda, O. Kitao, H. Nakai, T. Vreven, J. Montgomery, J. A. , J.E. Peralta, F. Ogliaro, M. Bearpark, J.J. Heyd, E. Brothers, K.N. Kudin, V.N. Staroverov, T. Keith, R. Kobayashi, J. Normand, K. Raghavachari, A. Rendell, J.C. Burant, S.S. Iyengar, J. Tomasi, M. Cossi, N. Rega, J.M. Millam, M. Klene, J.E. Knox, J.B. Cross, V. Bakken, C. Adamo, J. Jaramillo, R. Gomperts, R.E. Stratmann, O. Yazyev, A.J. Austin, R. Cammi, C. Pomelli, J.W. Ochterski, R.L. Martin, K. Morokuma, V.G. Zakrzewski, G.A. Voth, P. Salvador, J.J. Dannenberg, S. Dapprich, A.D. Daniels, O. Farkas, J.B. Foresman, J.V. Ortiz, J. Cioslowski and D.J. Fox, Gaussian 09, Gaussian Inc., Wallingford CT., 2013.
22. M.D. Hanwell, D.E. Curtis, D.C. Lonie, T. Vandermeersch, E. Zurek, G.R. Hutchison, *J. Cheminformatics*, **4**, 1 (2012).
23. R. Dennington, T. Keith and J. Millam, GaussView, Version 5, Semichem Inc., Shawnee Mission, KS, 2009.
24. T. Erdogan, F. Oguz Erdogan, *Lett. Org. Chem.*, **15**, 99 (2018).
25. J.B. Foresman, E. Frisch, Exploring Chemistry with Electronic Structure Methods. Second ed. Pittsburgh, PA: Gaussian, Inc., 1996.
26. H.K. Fun, S. Arshad, B. Garudachari, A.M. Isloor, M.N. Satyanarayan, *Acta Crystall., Section E-Structure Reports Online*, **67**, O1528-U1667 (2011).
27. T. Koopmans, *Physica*, **1**, 104 (1934).
28. P.K. Chattaraj, U. Sarkar D.R. Roy, *Chem. Reviews*, **106**, 2065 (2006).
29. R.S. Mulliken, *J. Chem. Phys.*, **2**, 782 (1934).
30. R.G. Parr, R.G. Pearson, *J. Amer. Chem. Soc.*, **105**, 7512 (1983).
31. R.G. Parr, L. Von Szentpaly, S.B. Liu, *Journal of the American Chemical Society*, **121**, p. 1922-1924 (1999).
32. R.G. Pearson, *J. Amer. Chem. Soc.*, **85**, 3533 (1963).
33. R.G. Pearson, *J. Chem. Educ.*, **45**, 581 (1968).
34. R.G. Pearson, *J. Chem. Educ.*, **76**, 267 (1999).
35. G. Makov, *J. Phys. Chem.*, **99**, 9337 (1995).